J. Fluid Mech. (2016), *vol.* 805, R3, doi:10.1017/jfm.2016.576

JFM RAPIDS
journals.cambridge.org/rapids

Observation of resonant interactions among surface gravity waves

F. Bonnefoy[1,†], F. Haudin[2], G. Michel[3], B. Semin[3], T. Humbert[4], S. Aumaître[4], M. Berhanu[2] and E. Falcon[2]

[1]École Centrale de Nantes, LHEEA, UMR 6598 CNRS, F-44 321 Nantes, France

[2]Univ. Paris Diderot, Sorbonne Paris Cité, MSC, UMR 7057 CNRS, F-75 013 Paris, France

[3]École Normale Supérieure, LPS, UMR 8550 CNRS, F-75 005 Paris, France

[4]Univ. Paris-Scalay, CEA-Saclay, SPEC, DRF, UMR 3680 CNRS, F-91 191 Gif-sur-Yvette, France

(Received 3 July 2016; revised 27 July 2016; accepted 27 August 2016; first published online 20 September 2016)

We experimentally study resonant interactions of oblique surface gravity waves in a large basin. Our results strongly extend previous experimental results performed mainly for perpendicular or collinear wave trains. We generate two oblique waves crossing at an acute angle, while we control their frequency ratio, steepnesses and directions. These mother waves mutually interact and give birth to a resonant wave whose properties (growth rate, resonant response curve and phase locking) are fully characterized. All our experimental results are found in good quantitative agreement with four-wave interaction theory with no fitting parameter. Off-resonance experiments are also reported and the relevant theoretical analysis is conducted and validated.

Key words: surface gravity waves, waves/free-surface flows

1. Introduction

Resonant interactions between nonlinear waves are an efficient mechanism to transfer energy between scales. For instance, three-wave interactions appear in various systems involving quadratic nonlinearity, such as for optical waves, hydrodynamic capillary surface waves, or elastic waves on a thin plate.

For hydrodynamic systems, experimental studies of three-wave interactions have been investigated for capillary surface waves (McGoldrick 1970; Henderson & Hammack 1987; Aubourg & Mordant 2015; Haudin *et al.* 2016), internal waves in stratified fluids (Martin, Simmons & Wunsch 1972; Joubaud *et al.* 2012) and inertial waves in fluids in rotation (Bordes *et al.* 2012). For wave systems involving concave dispersion relation (i.e. when the wave frequency ω follows $\omega(k) \sim k^{\nu}$

† Email address for correspondence: felicien.bonnefoy@ec-nantes.fr

with k the wavenumber and $\nu < 1$) or cubic nonlinearity, such as for surface gravity waves in deep water, three-wave resonance conditions cannot be fulfilled. Four-wave interactions may then occur if interacting waves fulfil the following resonance conditions $\boldsymbol{k}_1 + \boldsymbol{k}_2 = \boldsymbol{k}_3 + \boldsymbol{k}_4$ and $\omega_1 + \omega_2 = \omega_3 + \omega_4$, the angular frequencies ω_i and wavevectors $\boldsymbol{k}_i$ being linked by the linear wave dispersion relation $\omega_i \equiv \omega(\boldsymbol{k}_i)$. Mainly for the sake of simplicity, special attention has been given to the case of two degenerated mother waves, i.e. $\boldsymbol{k}_2 = \boldsymbol{k}_1$. Four-wave resonance conditions thus reduce to

$$\left.\begin{aligned} 2\boldsymbol{k}_1 - \boldsymbol{k}_3 &= \boldsymbol{k}_4, \\ 2\omega_1 - \omega_3 &= \omega_4, \end{aligned}\right\} \tag{1.1}$$

meaning that two interacting large-scale mother waves (1 and 3) can give birth to a smaller-scale daughter wave (4). Hereafter, we will focus only on surface gravity waves in deep water of linear dispersion relation

$$\omega(\boldsymbol{k}) = \sqrt{g|\boldsymbol{k}|}. \tag{1.2}$$

Four-wave interactions studies started in the early theoretical works of Phillips (1960) and Longuet-Higgins (1962). Surprisingly, there exist only few experiments specifically devoted to studying such resonant wave interactions between water waves. Longuet-Higgins & Smith (1966) and McGoldrick *et al.* (1966) were the first to observe the generation of a daughter wave by wave interactions in the degenerated case. They notably evidenced a linear growth rate of the daughter wave, at short propagation distance, as predicted theoretically (Longuet-Higgins 1962). These pioneering works were restricted to perpendicular mother waves with fixed and strong wave steepness ($ka = 0.1$, with a the wave amplitude) within a relatively small basin (3 m). In the same perpendicular configuration, Tomita (1989) confirmed the daughter growth rate to greater distances within a larger basin (54 m), still for fixed, but lower, mother-wave steepness ($ka < 0.05$). He also conducted slightly off-resonance experiments (wavenumber a few % apart from the resonance). In all those experiments, three degenerated waves of the interacting quartet are generated mechanically (mother waves) and the fourth one (daughter wave) is growing due to four-wave interaction. Finally, the non-degenerated case was conducted recently to observe finite amplitude effects on the resonance condition leading to persistent wave patterns (Hammack, Henderson & Segur 2005; Liu *et al.* 2015). In Liu *et al.* (2015), an experimental investigation of steady-state resonant waves is carried out for short-crested waves. A nonlinear steady-state quartet is obtained theoretically in the resonance condition by means of the homotopy analysis method. This quartet is then mechanically generated and the steady regime is indeed observed along the propagation in the basin. These experiments confirm the existence of steady-state resonant waves. In these experiments of Liu *et al.* (2015), the generated wave field consists of the four waves involved in the quartet plus some required higher-order waves, and therefore no daughter wave is expected in this case. More recently, Waseda *et al.* (2015) investigated experimentally the case of resonant interactions in the presence of an underwater current. Most of these observations were supported by a dynamic model for nonlinear wave interactions (Zakharov 1968; Krasitskii 1994). Note that another type of four-wave interactions involving collinear waves was extensively studied experimentally in the case of modulational instability (Benjamin–Feir instability) and focused on the growth of side-band satellites (Lake & Yuen 1977; Su *et al.* 1982; Shemer & Chamesse 1999; Tulin & Waseda 1999). Such an instability is not observable in our configuration.

Here, we performed experiments to study resonant interactions between two oblique surface gravity waves in a large basin in the degenerated case. Like Longuet-Higgins & Smith (1966), McGoldrick *et al.* (1966) and Tomita (1989) we generate three mother waves of a resonant quartet and we observe the growth of the fourth wave – the daughter wave. For the first time however, our experiments are carried out with mother waves crossing with an acute angle instead of perpendicular mother waves. The mother-wave frequency ratio, their interaction angle and steepnesses are control parameters. We fully characterized the generation of a daughter wave for resonance conditions (growth rate, resonance response curve with angle, and phase locking between resonant waves), as well as for out-of-resonance conditions (detuning factor). All our measurements are found in quantitative agreement with four-wave interaction theory with no fitting parameter, provided that the mother-wave steepnesses are small enough ($ka < 0.1$). We also provide theoretical explanations of the phase-locking mechanism and the off-resonance detuning factor from the dynamical equations of Zakharov (1968). The article is organized as follows. We first recall the resonant interaction theory, a perturbative approach only valid for short times (Phillips 1960; Longuet-Higgins 1962), and then we present the main predictions of the dynamical equations. Details of the derivation are given in the supplementary material available online at http://dx.doi.org/10.1017/jfm.2016.576. We introduce the experimental set-up, report the experimental results for resonant conditions, and for out-of-resonance conditions, before drawing our conclusions.

2. Perturbation approach of the resonant interaction theory

Phillips (1960) and Longuet-Higgins (1962) have investigated four-wave degenerated resonant solutions of (1.1) for deep-water waves. A 3D representation of the solutions for a given wavevector $\boldsymbol{k}_1$ is shown in figure 1 (see Aubourg & Mordant (2015) for gravity–capillary waves). The dashed black line is exactly the classical figure-of-eight given by Phillips (1960). The angle between a pair $\boldsymbol{k}_1$ and $\boldsymbol{k}_3$ on the figure-of-eight is denoted θ. The figure of eight is symmetric with respect to the $\boldsymbol{k}_1$ axis and either the frequency ratio $r = \omega_1/\omega_3$ or the angle θ may serve as a unique parameter to describe the figure-of-eight. A typical example quartet is drawn in blue vectors for the mother waves and magenta for the daughter wave; it corresponds to the maximal growth rate for $r = r_m = 1.258$.

Longuet-Higgins (1962) studied theoretically the degenerated resonance in a perturbation approach considering that the mother-wave amplitudes are unaffected by the growth of the daughter wave. Longuet-Higgins (1962) showed that the daughter-wave amplitude at resonance a_4^{res} follows

$$a_4^{res} = \varepsilon_1^2 \varepsilon_3 d G(r), \tag{2.1}$$

where ε_i are the steepnesses defined by $\varepsilon_i = k_i a_i$, a_i the wave amplitude, d is the distance from the wavemaker along the direction of the daughter wave and G a theoretical growth rate depending on the frequency ratio $r = \omega_1/\omega_3$. Note that the resonance conditions (1.1) in deep water provide for each r a unique angle θ; G may then be defined as a function of r or θ via $r(\theta)$. The resonant daughter wave is expected to grow linearly with distance and (2.1) remains valid as long as $a_4 \ll a_1$ and a_3. The growth rate G is shown in figure 2(*a*), as a function of the angle θ. For clarity, we have chosen positive angles for $r > 1$ and negative angles for $r < 1$. The growth rate is maximum for $\theta = \theta_m = 25^\circ$ ($r = r_m = 1.258$); we locate our experimental

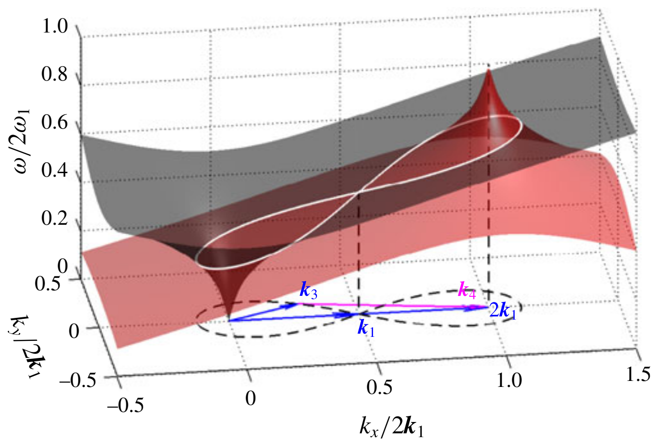

FIGURE 1. Solutions for four-wave resonances of surface gravity waves in the degenerated case of conditions (1.1). The dark-grey surface corresponds to $\omega(\boldsymbol{k}_3)$, i.e. (1.2) with $\boldsymbol{k}_3 = (k_x, k_y)$ and the red (light-grey) surface to the difference $2\omega(\boldsymbol{k}_1) - \omega(2\boldsymbol{k}_1 - \boldsymbol{k}_3)$ for a given $\boldsymbol{k}_1$. Resonance conditions (1.1) are located on the intersection of both surfaces (white solid line). Dashed line at the bottom of the axes corresponds to the projection of the white line. Example vectors are given for $f_1 = 0.9$ Hz, $f_3 = 0.714$ Hz and $\theta = \theta_m = 25°$.

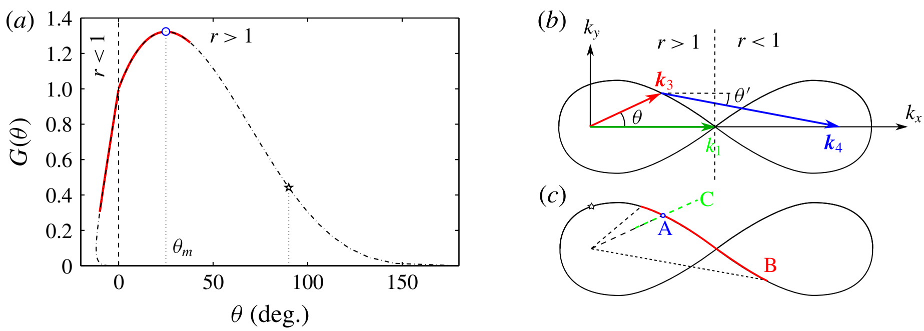

FIGURE 2. (*a*) Theoretical growth rate $G(\theta)$ of the daughter wave for the degenerated case (dash-dotted lines) and experimental tests studied in this paper: set A (blue circle), set B (red solid thick line) and experiments in litterature (black star). (*b*) Figure-of-eight with wavevectors. (*c*) Location of the experimental tests studied in this paper: resonant experiments: same convention as in (*a*) with letters A and B, off-resonance experiments: set C (green dashed line).

work around this angle θ_m to obtain a significant daughter-wave amplitude; the angle θ ranges from $-15°$ to $+40°$ in our experiments. The black star on the graph of figure 2 identifies the parameters used for the experiments of Longuet-Higgins & Smith (1966), McGoldrick *et al.* (1966) and Tomita (1989), which were all performed at $\theta = 90°$.

In Longuet-Higgins (1962), we can infer from the sine function describing the daughter wave and the cosine functions describing the mother waves that the phase of the daughter wave is locked to $-\pi/2$ with respect to the mother waves.

For out-of-resonance mother waves, Longuet-Higgins (1962) assumes that the daughter-wave resonant growth rate is modified by a factor $\sin(\Delta kd)/\Delta kd$, which was confirmed by later experiments (Longuet-Higgins & Smith 1966; McGoldrick *et al.* 1966), Δk being the wavenumber mismatch in resonance conditions (1.1). The Hamiltonian formulation given below provides a simple explanation for such a factor.

3. Hamiltonian formulation of the resonant interaction theory

Here, we use the framework of the approximate Hamiltonian theory of Zakharov (1968) with the formalism from Janssen (2009) in order to explain the off-resonance mismatch factor. The details of the derivation are left to the supplementary material in Bonnefoy *et al.* (2015). We apply the Hamiltonian theory to a resonant degenerated interaction with two mother waves (1 and 3), present initially, and a daughter wave (4) which grows in time. The wave action amplitude is $B(\boldsymbol{k}, t) = B_1(t)\delta(\boldsymbol{k}-\boldsymbol{k}_1) + B_3(t)\delta(\boldsymbol{k}-\boldsymbol{k}_3) + B_4(t)\delta(\boldsymbol{k}-\boldsymbol{k}_4)$, with the resonance condition $2\boldsymbol{k}_1 - \boldsymbol{k}_3 - \boldsymbol{k}_4 = \boldsymbol{0}$, and the linear frequency mismatch or detuning is $\Delta\omega = 2\omega_1 - \omega_3 - \omega_4$. The Zakharov equation leads to the following evolution equation for the wave action amplitudes $B_i(t)$ of the degenerated quartet

$$\mathrm{i}\partial_t B_1 = (\Omega_1 - \omega_1)B_1 + 2T_{1134}\exp(\mathrm{i}\Delta\omega t)B_1^* B_3 B_4, \tag{3.1a}$$

$$\mathrm{i}\partial_t B_3 = (\Omega_3 - \omega_3)B_3 + T_{1134}\exp(-\mathrm{i}\Delta\omega t)B_1^2 B_4^*, \tag{3.1b}$$

$$\mathrm{i}\partial_t B_4 = (\Omega_4 - \omega_4)B_4 + T_{1134}\exp(-\mathrm{i}\Delta\omega t)B_1^2 B_3^*. \tag{3.1c}$$

The interaction coefficients $T_{1234} = T(\boldsymbol{k}_1, \boldsymbol{k}_2, \boldsymbol{k}_3, \boldsymbol{k}_4)$ are the kernels given in Krasitskii (1994) or Janssen (2009). Nonlinear frequencies Ω_i satisfy the following nonlinear dispersion relations

$$\left.\begin{aligned} \Omega_1 &= \omega_1 + T_{1111}|B_1|^2 + 2T_{1313}|B_3|^2 + 2T_{1414}|B_4|^2, \\ \Omega_3 &= \omega_3 + 2T_{1313}|B_1|^2 + T_{3333}|B_3|^2 + 2T_{3434}|B_4|^2, \\ \Omega_4 &= \omega_4 + 2T_{1414}|B_1|^2 + 2T_{3434}|B_3|^2 + T_{4444}|B_4|^2. \end{aligned}\right\} \tag{3.2}$$

In the early stage of the resonant interaction or for a non-resonant interaction, the daughter-wave amplitude is assumed to be negligible with respect to the mother-wave amplitudes. Equations (3.1*a*) and (3.1*b*) give constant magnitude and slowly evolving phase for the mother waves while (3.1*c*) admits the following solution

$$B_4 = -\mathrm{i}T_{1134}B_{10}^2 B_{30}^* \frac{\sin(\Delta\Omega t/2)}{\Delta\Omega/2}\exp(-\mathrm{i}(\Omega_4 - \omega_4 + \Delta\Omega/2)t), \tag{3.3}$$

where the subindex 0 denotes the initial value and the total detuning is $\Delta\Omega = 2\Omega_1 - \Omega_3 - \Omega_4$. Derivation of this solution is straightforward and left to the supplementary material. Converting to wave amplitude by means of the relation $a_i = \sqrt{2k_i/\omega_i}B_i$, we can infer the following wave solutions.

At short times, when $|a_4| \ll |a_{10}|, |a_{30}|$, we obtain constant mother amplitudes $a_i(t) = a_{i0}$ (subindex 0 means initial value). The daughter-wave amplitude and phase are

$$|a_4| = T_{1134}\frac{\omega_1}{2k_1^3}\sqrt{\frac{\omega_3 k_4}{\omega_4 k_3^3}}\varepsilon_1^2\varepsilon_3\left|\frac{\sin(\Delta\Omega t/2)}{\Delta\Omega/2}\right|, \tag{3.4a}$$

$$\arg a_4 = -\frac{\pi}{2} + 2\arg a_{10} - \arg a_{30} - (\Omega_4 - \omega_4 + \Delta\Omega/2)t, \tag{3.4b}$$

where the steepness is defined by its initial value $\varepsilon_i = k_i|a_{i0}|$. Equation (3.4a) provides the evolution of the daughter-wave amplitude while (3.4b) gives the nonlinear evolution of its phase.

At resonance ($\Delta\omega = 0$) and at short times ($\Delta\Omega t \ll 1$), we have $\sin(\Delta\Omega t/2)/(\Delta\Omega/2) \simeq t$. Equation (3.4a) now becomes $|a_4^{res}| = T_{1134}\omega_1\sqrt{\omega_3 k_4}/(2k_1^3\sqrt{\omega_4 k_3^3})\varepsilon_{10}^2\varepsilon_{30}t$, which corresponds to the same results as in Longuet-Higgins (1962). Equation (3.4b) shows that the daughter-wave phase is phase-locked to $\arg a_{40} = -\pi/2 + 2\arg a_{10} - \arg a_{30}$.

In the case of mechanically generated mother waves, the daughter-wave frequency follows from the exact resonance condition $\omega_4 = 2\omega_1 - \omega_3$. It is necessary to replace time t in (3.4) by d/c_{g4}, where c_{g4} is the group velocity of the daughter wave and d the distance in the daughter-wave direction. All the following results are valid in the steady regime between the wavemaker and the daughter-wavefront. At resonance, the theoretical amplitude of the resonant wave along the basin is the same as in (2.1) (the link between G and T_{1134} is given in the supplementary material).

We consider now an off-resonance degenerated quartet with a linear frequency detuning $\Delta\omega \neq 0$. At the early stage of the interaction, when the daughter amplitude is small compared to the mother amplitudes, expression (3.4a) shows that the daughter amplitude evolves as a sine function. We may rewrite (3.4a) as $|a_4| = |a_4^{res}|\operatorname{sinc}\Delta\Omega t/2$. Note that this mismatch factor involves the total detuning $\Delta\Omega$, which consists of both linear and nonlinear components. At longer times, the phase mismatch will change from its initial $\Delta\omega$ value due to nonlinear dispersion. For off-resonant mechanically generated mother waves, the direction θ_4 of the daughter wavenumber $\boldsymbol{k}_4$ is yet unknown; the condition for wavenumbers is not fulfilled and a wavevector mismatch exists, $\Delta\boldsymbol{k} = 2\boldsymbol{k}_1 - \boldsymbol{k}_3 - \boldsymbol{k}_4$. Although the direction of the daughter wave is not specified, we assume that the fastest growing daughter wave is the one with minimal detuning. In other words, the daughter wave propagates along the direction of $2\boldsymbol{k}_1 - \boldsymbol{k}_3$ and the corresponding mismatch is now $\Delta k = |2\boldsymbol{k}_1 - \boldsymbol{k}_3| - k(2\omega_1 - \omega_3)$. From (3.4a), the off-resonance amplitude of the daughter wave is given by the same expression as in Longuet-Higgins (1962)

$$a_4 = \varepsilon_1^2\varepsilon_3 d G(r,\theta)\left|\frac{\sin\frac{1}{2}\Delta k d}{\frac{1}{2}\Delta k d}\right| = a_4^{res}\left|\operatorname{sinc}\frac{\Delta k d}{2}\right|. \tag{3.5}$$

Note that the nonlinear detuning terms have been omitted here for clarity.

4. Experimental set-up

The experiments presented here are designed to test the resonance theory for wave directions different from the perpendicular case studied in the 1960s and by Tomita (1989). We mechanically generate bichromatic waves (mother waves 1 and 3) in a rectangular wave basin and observe the birth of the daughter wave of frequency $2\omega_1 - \omega_3$ due to resonant interaction (see the supplementary movie available online at http://dx.doi.org/10.1017/jfm.2016.576). The wave basin at Ecole Centrale de Nantes has dimensions 50 m × 30 m × 5 m and its wavemaker consists of 48 independant flaps that are hinged 2.8 m below the free surface. Figure 3(a) shows a top view of the set-up. In order to avoid spurious reflections on the sidewalls, the motion of the segmented wavemaker is controlled by means of the Dalrymple method (Dalrymple 1989). The Dalrymple method aims at generating the target wave field at a distance $X_d = 10$ m from the wavemaker and yields a quasi-uniform wave field from the wavemaker up to 25 m (see the grey zone of figure 3a); this is crucial for these interaction experiments.

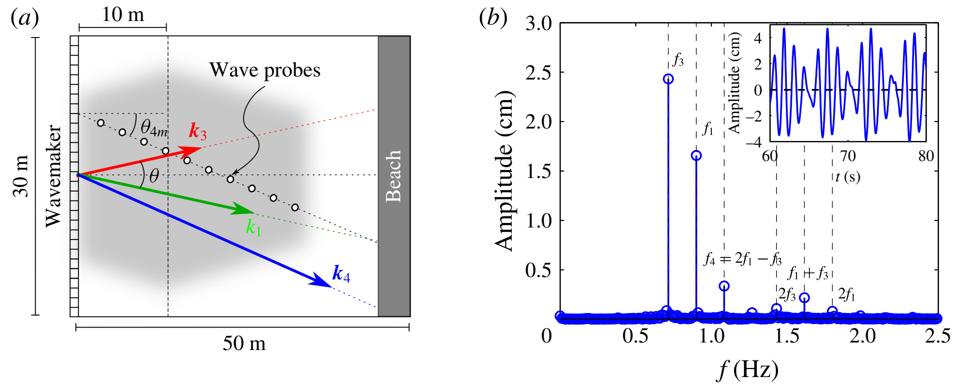

FIGURE 3. (a) Wave basin showing the homogeneous zone (shaded area), the wave probes (circles) and the wavevectors $\boldsymbol{k}_1$, $\boldsymbol{k}_3$ and $\boldsymbol{k}_4$ for the maximum growth rate case (arrows respectively in green, red and blue); (b) frequency spectrum of wave height $a(t)$ recorded at $d = 21.5$ m. Vertical dashed lines correspond to frequencies: f_3, f_1, f_4, $2f_3$, $f_1 + f_3$, and $2f_1$. Inset: temporal evolution of the wave height, $a(t)$, dashed line is $\langle a \rangle_t \simeq 0$. Wave conditions $r = r_m$, $\theta = \theta_m$ and $\varepsilon_1 = \varepsilon_3 = 0.05$.

The input parameters to the wavemaker are mother-wave frequency (f_1 and f_3), steepness (or amplitude a_1 or a_3) and direction (θ_1 and θ_3 with respect to the basin main axis). The daughter-wave direction is defined as θ_4 in the wave basin. Frequencies for the mother waves are chosen to fit the basin capacities: fixed $f_1 = 0.9$ Hz (wavelength $\lambda_1 \simeq 2$ m) and varied $f_3 = f_1/r$ with $r = 0.8$–1.6. The corresponding wavelengths λ_3 ranged from 1.3 to 4 m. The angle $\theta = \theta_3 - \theta_1$ between mother waves 1 and 3 was varied between $-15°$ and $40°$ with a focus at $\theta_m = 25°$ where the maximum growth rate of the daughter wave occurs ($r_m = 1.258$, see figure 2). In this case, we have $\theta_4 = \theta_{4m} = -23.1°$.

Three sets of experiments are presented in the following, two at resonance and one out of resonance. In the first set of experiments, (set A corresponds to the point A in figure 2c), the scaling of the daughter-wave steepness ε_4 is tested by varying $\varepsilon_1 \in [0.01; 0.1]$ at the resonance condition with maximum growth rate (that is $r = r_m$) and for fixed $\varepsilon_3 = 0.05$. In set B, the figure-of-eight is tested in the range $\theta \in [-15°; 40°]$, for fixed steepnesses $\varepsilon_1 = \varepsilon_3 = 0.07$. This corresponds to the red line in figure 2(a) and on the figure-of-eight in figure 2(c). Finally, in set C, we study out-of-resonance conditions by fixing $f_1 = 0.9$ Hz and $\theta = \theta_m$ but changing k_3 by varying $r \in [1.1; 1.6]$ around r_m, again with fixed steepnesses $\varepsilon_1 = \varepsilon_3 = 0.05$. This corresponds to the dashed green line in figure 2(c).

For cases A and C, wave directions in the basin are made symmetrical $\theta_1 = -\theta_m/2$ and $\theta_3 = \theta_m/2$ to maximize the uniformity of the wave field. The direction of the daughter wave is $\theta_{4m} = -23.1°$, which corresponds to the cases A and C with maximum growth rate when $\theta = \theta_m$. A linear frame supporting an array of twelve resistive wave probes is set up in the direction θ_{4m} (see figure 3a). The distance between two successive probes is approximately 2 m. In all experiments, this linear array of wave probes is indeed aligned along the direction of the daughter wave $\theta_{4m} = -23.1°$. The distance d to the wavemaker and measured along the direction of the daughter wave ranges from $d = 2.5$ to 25 m.

For case B, the directions of the mother waves θ_1 and θ_3 were chosen in such a way that the target angle θ is obtained and that the daughter wave is aligned with the probe array.

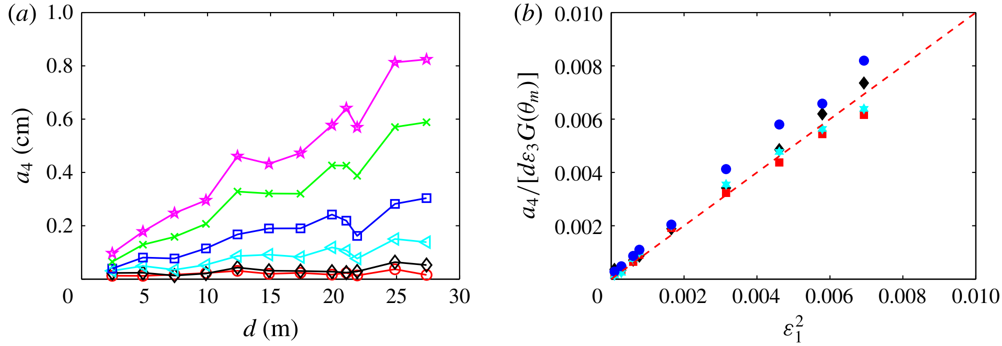

FIGURE 4. Amplitude of the resonant wave a_4 for $\varepsilon_3 = 0.05$ and $r = r_m$. (*a*) Amplitude a_4 versus distance, d, for different $\varepsilon_1 \times 10^3 = 10$, 17, 28, 41, 56, 68 (from bottom to top). (*b*) Rescaled amplitude of the resonant wave $a_4/[d\varepsilon_3 G(\theta_m)]$ as a function of ε_1^2 for different distances $d = 9.9$ (◆), 14.9 (■), 19.9 (∗), and 24.9 (●) m. The dashed line of unity slope is expected from (2.1).

The sampling frequency is 100 Hz. Wave heights were recorded during approximately 100 s, which corresponds to a steady regime of more than 50 wave periods. Typical amplitudes are $a_{1,3} \simeq$ few cm for mother waves and $a_4 \simeq$ few mm for daughter waves.

5. Resonant wave conditions

We report here our results for resonant degenerated quartets near maximum amplification (case A). A typical example of a temporal evolution of wave elevation $a(t)$ recorded by a probe is shown in the inset of figure 3(*b*). From the time series measured at the wave probes, we select a steady-state window after the wavefront passed the probe (time window is more than 50 periods long). A Discrete Fourier Transform is applied to the windowed signal with a standard FFT algorithm (frequency resolution is below 20 mHz). The main figure 3(*b*), shows the corresponding amplitude spectrum for case A. The two mother waves were visible at frequency f_1 and f_3. The peak at frequency $f_4 = 2f_1 - f_3$ confirms the existence of the daughter wave, but, as expected, its amplitude is smaller than those of the mother waves. This is a first piece of evidence for a daughter wave generated by resonant interaction. Note that harmonics at frequency $2f_3$, $f_1 + f_3$ and $2f_1$ are also visible, with amplitudes yet lower than that of the daughter wave. They are the signature of second-order bound waves accompanying the mother waves. The harmonics at $3f_3$ and $2f_3 - f_1$ corresponding to the third-order bound waves are barely visible.

Figure 4(*a*) shows the daughter-wave amplitude a_4 as a function of distance d for different steepnesses. This amplitude is found to grow linearly with distance d, as expected from (2.1), and to increase with the mother-wave steepness ε_1. Note that the experiments when ε_1 is fixed and ε_3 is varied (not shown here) show that the daughter amplitude a_4 grows linearly with ε_3 as predicted. The rescaled daughter-wave amplitude $a_4/(\varepsilon_3 d G(\theta_m))$ is then shown in figure 4(*b*) as a function of ε_1^2 at different distances d. A good quantitative agreement with the theoretical predictions of (2.1) is observed, with no fitting parameter.

For a given probe at the far end of the homogeneous zone, we separate the two mother waves and the daughter wave with appropriate bandpass filters around each

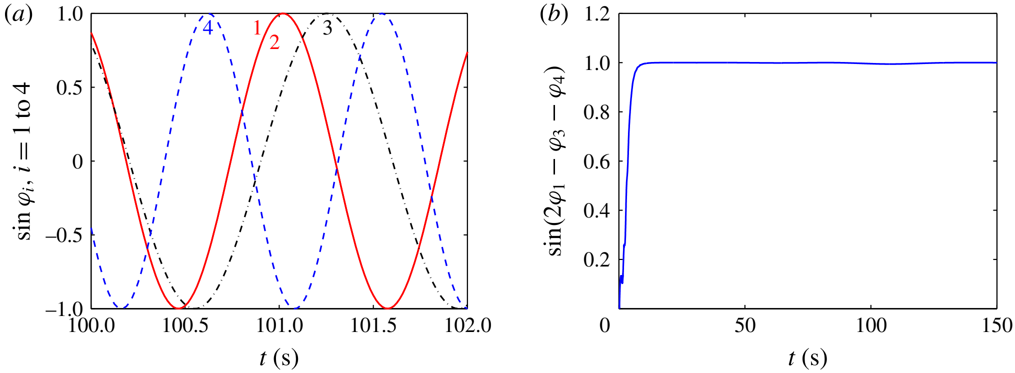

FIGURE 5. (a) Temporal evolution of the individual phase $\varphi_i(t) \equiv \boldsymbol{k}_i \boldsymbol{\cdot} \boldsymbol{x}_p - \omega_i t + \varphi_{i0}$ of each wave $i=1$ (——), 3 (–·–), and 4 (– – –). (b) Temporal evolution of the sine of the interaction phase $\varphi(t) = 2\varphi_1 - \varphi_3 - \varphi_4$. At resonance, the latter reduces to $2\varphi_{10} - \varphi_{30} - \varphi_{40}$, which is constant (phase locking) and equal to $\pi/2$ during the experiment. Conditions $r = r_m$, $\varepsilon_1 = \varepsilon_3 = 0.05$ at distance $d = 21.5$ m.

component f_1, f_3 and $2f_1 - f_3$. To wit, we compute the Hilbert transform of each component and we obtain the wave envelope $a_i(t)$ and instantaneous wave phase $\varphi_i(t) \equiv \boldsymbol{k}_i \boldsymbol{\cdot} \boldsymbol{x}_p - \omega_i t + \varphi_{i0}$, where $\boldsymbol{x}_p$ is the probe position. The phase of each wave $\varphi_i(t)$ is shown in figure 5(a) and obviously changes with time. In contrast, the interaction phase defined by $\varphi(t) = 2\varphi_1(t) - \varphi_3(t) - \varphi_4(t)$ is constant with time, as shown in figure 5(b). After the wavefront has passed the probes, the interaction phase φ is locked at $\pi/2$. This phase locking demonstrated by our experiments is in very good agreement with the phase locking predicted by (3.4b) for short distance (i.e. $a_4 \ll a_1$ and a_3). The steepness is small during this experiment, so the phase locking is visible even on the most distant probes. This phase locking is a second piece of evidence for the generation of the daughter wave by resonant interactions.

The figure-of-eight is now investigated in the vicinity of maximum growth rate (the thick red line in figure 2a). In the dedicated experiments B, the mother-wave angle θ is varied in the range from $-15°$ to $0°$ in the case $r < 1$ (or $f_3 > f_1$) and from $0°$ to $+40°$ in the case $r > 1$. For each angle θ, the frequency f_3 is chosen so that $\boldsymbol{k}_3$ is located on the figure-of-eight (see figure 2b,c) in order to fulfil the resonance conditions. Note that the correct choice of the directions θ_1 and θ_3 of the individual mother waves in the basin is a key point in obtaining significant results. The successful strategy is to ensure the direction of daughter wave 4 follows the line of the probes. Figure 6 shows the rescaled daughter-wave amplitude $a_4/(\varepsilon_1^2 \varepsilon_3 d)$ as a function of the angle θ for different distances d at fixed steepnesses ε_1 and ε_3. This rescaling allows one to measure experimentally the resonance response curve $G(\theta)$ predicted by Longuet-Higgins (1962). For all values of θ, a good quantitative agreement with the theoretical $G(\theta)$ is observed with no fitting parameter. This strongly extends previous experiments (Longuet-Higgins & Smith 1966; McGoldrick *et al.* 1966; Tomita 1989), which were carried out only for perpendicular conditions ($\theta = 90°$).

6. Out-of-resonance experiments

Let us now turn to experiments with out-of-resonance conditions for mechanically generated mother waves. These conditions correspond to $2\omega_1 - \omega_3 - \omega_4 = 0$ and

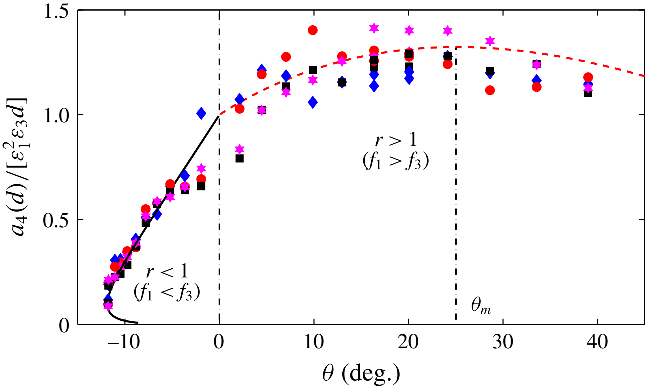

FIGURE 6. Rescaled amplitude $a_4/(\varepsilon_1^2\varepsilon_3 d)$ versus angle θ for different distances $d = 7.8$ (◆), 9.9 (●), 11.9 (■), and 13.8 (∗) m. Theoretical resonance curve $G[\theta(r)]$ for $r < 1$ (solid black line) and $r > 1$ (dashed red/grey line) from Longuet-Higgins (1962) (see also figure 2*a*). $\varepsilon_1 = \varepsilon_3 = 0.07$. $f_1 = 0.9$ Hz. $0.83 \leqslant r \equiv f_1/f_3 \leqslant 1.38$. $\theta_m = 25°$.

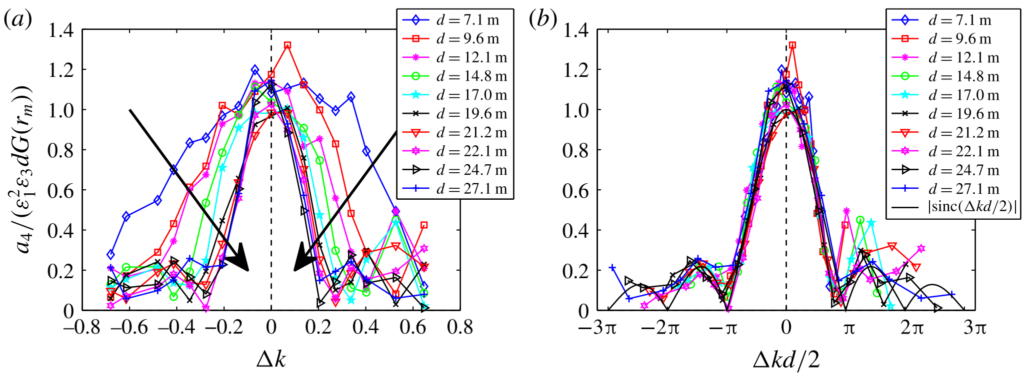

FIGURE 7. Rescaled amplitude $a_4/(\varepsilon_1^2\varepsilon_3 dG(r_m))$ measured at different distances d for out-of-resonance conditions ($\varepsilon_1 = \varepsilon_3 = 0.07$ and $f_1 = 0.9$ Hz). (*a*) Rescaled a_4 versus detuning Δk. Symbols correspond to different $d = 7$ up to 27 m (see arrows). (*b*) Rescaled a_4 versus normalized detuning $\Delta kd/2$. Solid line: absolute sinc function $|\mathrm{sinc}\Delta kd/2|$ from the Longuet-Higgins (1962) estimation or from (3.5).

$2\boldsymbol{k}_1 - \boldsymbol{k}_3 - \boldsymbol{k}_4 \equiv \Delta\boldsymbol{k} \neq \boldsymbol{0}$. Although the direction of the daughter wave is not specified, we assume that the fastest growing daughter wave is the one with minimal detuning. In other words, the daughter wave propagates along the direction of $2\boldsymbol{k}_1 - \boldsymbol{k}_3$ and the corresponding detuning is now $\Delta k \equiv |2\boldsymbol{k}_1 - \boldsymbol{k}_3| - k(2\omega_1 - \omega_3)$. We investigate experimentally this case (set C) near the location of the maximum growth rate at $r = r_m$. To wit, we kept the same angle $\theta = \theta_m$ and varied the frequency f_3 so that $\boldsymbol{k}_3$ can deviate from the figure-of-eight (see the green dashed line in figure 2*c*). Figure 7(*a*) shows the normalized daughter-wave amplitude defined by $a_4/(\varepsilon_1^2\varepsilon_3 dG(r_m))$ as a function of the detuning Δk for different distances d. We observe a decrease of the resonance bandwidth with increasing distance, as expected from the sinc term in (3.5). We rescaled all these curves on a single curve, as shown on figure 7(*b*), by scaling the detuning by half the distance. We observe that all our measurements collapse on the sinc curve, showing a good agreement with the estimation from Longuet-Higgins (1962) or from (3.5) rigorously derived.

7. Conclusion

We have presented experiments on resonant interactions of surface gravity waves within the Ecole Centrale de Nantes wave basin (50 m long by 30 m large by 5 m deep) in a degenerated case. Bichromatic mother waves were generated mechanically by means of specific control of oblique wave generation (Dalrymple method). The linear spatial growth of a resonant daughter wave was observed. The theoretical and experimental results presented here extend the pioneering work done in the 1960s. Four-wave interaction theory is expressed in the framework of Hamiltonian dynamic theory to demonstrate a phase-locking mechanism for resonant quartets and estimate the daughter-wave amplitude in nearly resonant quartets. All these theoretical results are supported by experimental observations of generated oblique mother waves: the observed linear spatial growth rate of daughter wave scaling with mother-wave steepness; the phase locking between resonant waves; the growth rate G satisfying the law historically found by Longuet-Higgins (1962); as well as the off-resonance response following the expected sinc curve.

The experiments presented in this article correspond to the early stage of resonance, that is when $k_4\varepsilon^2 d < 1$. Indeed, for longer distance or greater steepness, we observed other common features of nonlinear interactions at resonance (not reported in this paper) such as the pumping of the mother wave by the resonant wave and the decrease of the resonant-wave growth. For off-resonance conditions and stronger wave steepness ($ka > 0.1$), a departure from the approximate off-resonance (3.5) is observed: the distortion of the response curve (sinc) by a nonlinear detuning. These nonlinear effects will be the subject of a further publication. The Hamiltonian theory may serve as an extension of the theory in Longuet-Higgins (1962) to higher steepness, either by analytical solutions (see e.g. Stiassnie & Shemer 2005) or numerical solutions (Leblanc 2009). Finally, experiments with much greater steepness should make the quantification of the departure from weakly nonlinear theory (Zakharov equation) possible. It would also provide a better understanding of wave turbulence experiments in strongly nonlinear regimes.

Acknowledgements

This work was supported by ANR Turbulon 12-BS04-0005. We thank C. Laroche and A. Levesque for their technical help. We also thank H. Houtani and T. Waseda for providing us with the report by Tomita (1989).

Supplementary material and movie

Supplementary material and a movie are available at http://dx.doi.org/10.1017/jfm.2016.576.

References

AUBOURG, Q. & MORDANT, N. 2015 Nonlocal resonances in weak turbulence of gravity–capillary waves. *Phys. Rev. Lett.* **114**, 144501.

BONNEFOY, F., HAUDIN, F., MICHEL, G., SEMIN, B., HUMBERT, T., AUMAÎTRE, S., BERHANU, M. & FALCON, E. 2015 Other supplementary material, observation of resonant interactions among gravity surface waves.

BORDES, G., MOISY, F., DAUXOIS, T. & CORTET, P.-P. 2012 Experimental evidence of a triadic resonance of plane inertial waves in a rotating fluid. *Phys. Fluids* **24**, 014105.

DALRYMPLE, R. A. 1989 Directional wavemaker theory with sidewall reflection. *J. Hydraul. Res.* **27** (1), 23–24.

HAMMACK, J. L., HENDERSON, D. M. & SEGUR, H. 2005 Progressive waves with persistent two-dimensional surface patterns in deep water. *J. Fluid Mech.* **532**, 1–52.

HAUDIN, F., CAZAUBIEL, A., DEIKE, L., JAMIN, T., FALCON, E. & BERHANU, M. 2016 Experimental study of three-wave interactions among capillary–gravity surface waves. *Phys. Rev.* E **93**, 043110.

HENDERSON, D. M. & HAMMACK, J. L. 1987 Experiments on ripple instabilities. Part 1. Resonant triads. *J. Fluid Mech.* **184**, 15–41.

JANSSEN, P. A. E. M. 2009 On some consequences of the canonical transformation in the Hamiltonian theory of water waves. *J. Fluid Mech.* **637**, 1–44.

JOUBAUD, S., MUNROE, J., ODIER, P. & DAUXOIS, T. 2012 Experimental parametric subharmonic instability in stratified fluids. *Phys. Fluids* **24**, 041703.

KRASITSKII, V. P. 1994 On reduced equations in the Hamiltonian theory of weakly nonlinear surface waves. *J. Fluid Mech.* **272**, 1–20.

LAKE, B. & YUEN, H. 1977 A note on some nonlinear water–wave experiments and the comparison of data with theory. *J. Fluid Mech.* **83**, 75–81.

LEBLANC, S. 2009 Stability of bichromatic gravity waves on deep water. *Eur. J. Mech.* (B*/Fluids)* **28** (5), 605–612.

LIU, Z., XU, D. L., LI, J., PENG, T., ALSAEDI, A. & LIAO, S. J. 2015 On the existence of steady-state resonant waves in experiments. *J. Fluid Mech.* **763**, 1–23.

LONGUET-HIGGINS, M. S. 1962 Resonant interactions between two trains of gravity waves. *J. Fluid Mech.* **12**, 321–332. We have noticed a misprint in (6.4) in Longuet-Higgins (1962): the term $-(6+\xi^2)^{1/2}$ should be replaced by $-\text{sgn}(\xi)(6+\xi^2)^{1/2}$ where $\xi=(1-r)/r$.

LONGUET-HIGGINS, M. S. & SMITH, N. D. 1966 An experiment on third-order resonant wave interactions. *J. Fluid Mech.* **25**, 417–435.

MARTIN, B. S., SIMMONS, W. & WUNSCH, C. 1972 The excitation of resonant triads by single internal waves. *J. Fluid Mech.* **53**, 17–44.

MCGOLDRICK, L. F. 1970 An experiment on second-order capillary gravity resonant wave interactions. *J. Fluid Mech.* **40**, 251–271.

MCGOLDRICK, L. F., PHILLIPS, O. M., HUANG, N. E. & HODGSON, T. H. 1966 Measurements of third-order resonant wave interactions. *J. Fluid Mech.* **25**, 437–456.

PHILLIPS, O. M. 1960 On the dynamics of unsteady gravity waves of finite amplitude. Part I. The elementary interactions. *J. Fluid Mech.* **9**, 193–217.

SHEMER, L. & CHAMESSE, M. 1999 Experiments on nonlinear gravity–capillary waves. *J. Fluid Mech.* **380**, 205–232.

STIASSNIE, M. & SHEMER, L. 2005 On the interaction of four water–waves. *Wave Motion* **41** (4), 307–328.

SU, M.-Y., BERGIN, M., MARLER, P. & MYRICK, R. 1982 Experiments on nonlinear instabilities and evolution of steep gravity–wave trains. *J. Fluid Mech.* **124**, 45–72.

TOMITA, H. 1989 Theoretical and experimental investigations of interaction among deep-water gravity waves. *Rep. Ship Res. Inst.* **26** (5), 251–350.

TULIN, M. P. & WASEDA, T. 1999 Laboratory observations of wave group evolution, including breaking effects. *J. Fluid Mech.* **378**, 197–232.

WASEDA, T., KINOSHITA, T., CAVALERI, L. & TOFFOLI, A. 2015 Third-order resonant wave interactions under the influence of background current fields. *J. Fluid Mech.* **784**, 51–73.

ZAKHAROV, V. 1968 Stability of periodic waves of finite amplitude on a surface of a deep fluid. *J. Appl. Mech. Tech. Phys.* **2**, 190–198.